Journal of Alloys and Compounds 480 (2009) 28–30

Contents lists available at ScienceDirect

Journal of Alloys and Compounds

journal homepage: www.elsevier.com/locate/jallcom

Anisotropic magnetism in $PrCrSb_3$ and $NdCrSb_3$

Manjusha Inamdar, A. Thamizhavel, S. Ramakrishnan*

Tata Institute of Fundamental Research, Homi Bhabha Road, Mumbai 400 005, India

ARTICLE INFO

Article history:
Received 19 June 2008
Received in revised form
16 September 2008
Accepted 17 September 2008
Available online 21 November 2008

PACS:
61.66.−f
61.66.Dk
61.05.cp
71.20.Lp (examples)

Keywords:
$RCrSb_3$
Flux growth
Ferromagnetism

ABSTRACT

In this work we compare resistivity, susceptibility, magnetization and heat capacity of single crystals of $PrCrSb_3$ and $NdCrSb_3$. Both of them exhibit ferromagnetic ordering of Cr moments at 112 K and 100 K, respectively. Pr and Nd moments order at low temperatures ($T_N^{Pr} = 12$ K and $T_C^{Nd} = 10$ K) leading to moment compensation effects, even though bulk ferromagnetism of Cr moments persists down to the lowest temperature. The transport studies on $PrCrSb_3$ show existence of gap in the spin-wave spectrum which seems to be absent in $NdCrSb_3$. Moreover, the observed anisotropy in bulk properties and the ferromagnetic ordering of Cr moments are found to decrease with decrease in the size of the rare earth ion.

1. Introduction

$RCrSb_3$ crystallizes in orthorhombic structure, space group Pbcm [1]. It has a quasi two-dimensional structure with RSb and $CrSb_2$ layers stacked perpendicular to *a*-axis. $RCrSb_3$ is one of the few systems where one could study the interplay of 3d and 4f moments resulting in an interesting magnetic phase diagram. Moreover, it is conjectured that Cr has both local and itinerant character in $LaCrSb_3$ [2]. The itinerant Cr moments order ferromagnetically (FM) at 123 K whereas the local Cr moments order antiferromagnetically (AFM) at 96 K. This dual character of Cr moments is not seen in other members of the series. However, magnetic phase diagram enriches appreciably with La being replaced by other rare earth ions in this series due to non-zero moment contribution from these ions to the magnetic ordering of the compound. The next member, $CeCrSb_3$ shows one sharp anomaly in magnetization at 115 K due to FM ordering of Cr moments [3,4]. Although we do not see any sharp magnetic ordering due to Ce moments but its presence in $CeCrSb_3$ changes the magnetic phase diagram considerably as compared to that of $LaCrSb_3$. Unlike $CeCrSb_3$ we see a low temperature magnetic ordering due to rare earth moments in $PrCrSb_3$ and $NdCrSb_3$ along with high temperature FM due to Cr moments. Pr orders AFM at 12 K and Nd orders FM at 10 K. This paper presents a comparison between the magnetic and transport properties of these two systems.

2. Experimental details

Single crystals of $PrCrSb_3$ and $NdCrSb_3$ were grown by self-flux method. The phase was confirmed by performing powder X-ray diffraction on few grounded crystals. The Rietveld refinement of the X-ray pattern resulted in an orthorhombic lattice constants $a = 13.011(9)$ A, $b = 6.169(7)$ A and $c = 6.063(1)$ A for $PrCrSb_3$ and $a = 12.955(5)$ A, $b = 6.164(4)$ A and $c = 6.052(2)$ A for $NdCrSb_3$. From Laue back scattering pictures the largest surface was found to be the *bc*-plane.

The temperature dependence of the magnetic susceptibility $\chi(T)$ along the individual axis was measured using a commercial SQUID magnetometer (MPMS5, Quantum Design, USA). The resistivity $\rho(T)$ between 1.5 K and 300 K was measured using an LR700 resistance bridge (Linear Research, USA) by the 4-probe method with contacts made using silver paste. The heat capacity $C_p(T)$ in zero field between 5 K and 200 K was measured using the commercial PPMS (Quantum Design, USA).

3. Results and discussions

Fig. 1 shows data from the anisotropic dc susceptibility $\chi(T)$ measurements along the three principal directions, *a*, *b* and *c* for both the crystals for temperature between 4.2 K and 300 K in a field of 0.1 T. In Panel A we see susceptibility for $PrCrSb_3$ along all axes show a sharp anomaly at $T_C = 112$ K. This anomaly is attributed to ferromagnetic ordering of Cr moments as also seen in $LaCrSb_3$ at

* Corresponding author. Tel.: +91 22 22782302; fax: +91 22 804747.
E-mail address: ramky@tifr.res.in (S. Ramakrishnan).

0925-8388/$ – see front matter © 2008 Elsevier B.V. All rights reserved.
doi:10.1016/j.jallcom.2008.09.186

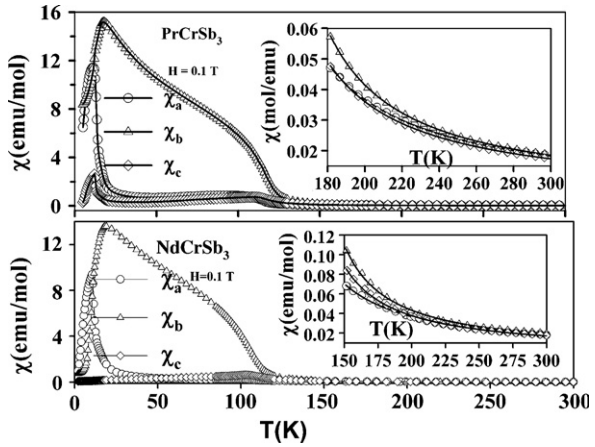

Fig. 1. The susceptibility versus temperature data $\chi(T)$ down to 2 K along all the three axes is shown in top(bottom) panel for $PrCrSb_3$($NdCrSb_3$). The insets in both panels show high temperature fit to the modified Curie–Wiess law.

123 K. The anisotropy in the magnetic property of this system is evident as we see the ratio χ_b/χ_a is almost 1.2 and χ_b/χ_c is 27 below 5 K. The large value of χ along b suggests that b is an easy axis for Cr moments. Below T_C the magnetic phase diagram seems complicated. As signature of $\chi(T)$ along b-axis is different than it is along a- and c-axes. Pr moments seem to couple AFM with Cr resulting in a dip kind of feature between T_C and T_N. At T_N we see a sharp drop in $\chi(T)$ along all the axes. This drop is attributed to the ordering of Pr moments.

The magnetic phase diagram for $NdCrSb_3$, shown in panel B of Fig. 1 looks very similar to that of $PrCrSb_3$. Like all previous members of the series here too b continues to be the easy axis of magnetization for Cr moments, which order ferromagnetically at $T_C = 100$ K. The sharp low temperature anomaly at $T_C^{Nd} = 10$ K along all the axes is signature for ordering of Nd moments.

The insets in both the panels are high temperature fits to the modified Curie–Wiess law, $\chi(T) = \chi_o + C/T - \Theta$. The value of χ_o is of the order of 10^{-3} emu/mol for the systems. The Curie constant gives effective moment of $4.24\mu_B$ for $PrCrSb_3$ and $5.2\mu_B$ for $NdCrSb_3$ as compared to $3.01\mu_B$ for $LaCrSb_3$. The value of Θ is positive as expected for ferromagnets and is about 130 K and 115 K, respectively for (Pr and Nd)$CrSb_3$ along all the axes.

For further understanding of magnetic properties of both the systems we have performed the isothermal magnetization measurements along all the three axes. As seen in Fig. 2 both $PrCrSb_3$ and $NdCrSb_3$ remain ferromagnetic down to lowest temperature. The magnetization appears hysteretic (not shown here for brevity) along all the axes at 2 K. The magnetization along a- and b-axes for $PrCrSb_3$($NdCrSb_3$) saturate to $3.63(4.2)\mu_B$ and $3.75(3.7)\mu_B$ respectively as compared to the saturation moment of $1.5\mu_B$ for $LaCrSb_3$ [2]. The saturation moment has contribution both from R^{3+} and Cr^{3+} ions. The moments along c-axis do not saturate till 12 T of field. The high value of moments along a-axis suggest that a is the easy axis for both Pr and Nd moments. We also see field induced cross-over for Pr easy axis from a- to b-axes at 6 T.

The resistivity versus temperature data for the $PrCrSb_3$ is shown in top panel of Fig. 3 for temperature between 1.5 K and 300 K for excitation current I along a- and b-axes. As expected the resistivity shows sharp fall in $\rho(T)$ at T_C due to the decrease in the spin-disorder scattering at ferromagnetic transition. The sample thickness was too small along c-axis so the resistive measurement along it was difficult and is not reported here. $PrCrSb_3$ exhibits high anisotropy in resistivity with room temperature values of

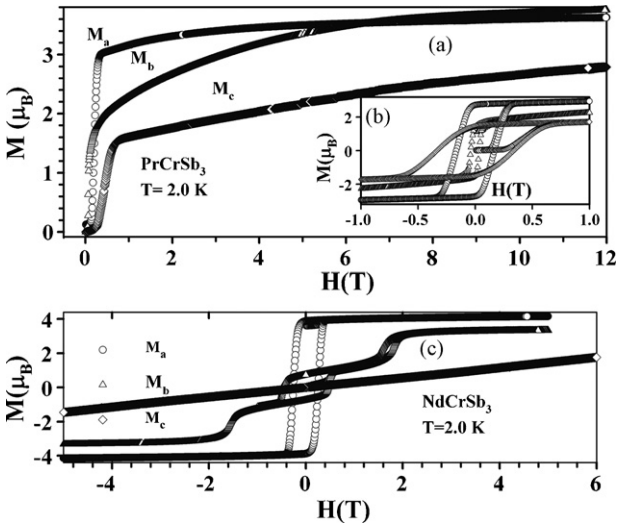

Fig. 2. The top panel shows isothermal magnetization $M(H)$ for $PrCrSb_3$ at 2 K along all the three axes. The lower panel gives $M(H)$ data for $NdCrSb_3$ sample at 2 K.

$\rho_a = 903\ \mu\Omega$ cm, $\rho_b = 148\ \mu\Omega$ cm and $\rho_c = 106\ \mu\Omega$ cm. The observed anisotropy is comparable to that observed in other $RCrSb_3$ crystals. We also see a sharp fall in $\rho(T)$ at $T_N = 12$ K, which again can be explained by decrease in spin-disorder scattering due to magnetic order. The inset of the top panel shows the low temperature resistivity fitted to the expression

$$\rho(T) = \rho_0 + aT^2 + bT\,\Delta\left[\frac{1+2T}{\Delta}\right]\exp\left(-\frac{\Delta}{T}\right)$$

where ρ_0 is residual resistivity, a is coefficient for electron–electron scattering, b is coefficient responsible for electron–magnon scattering and Δ is gap in spin-wave spectrum for the ferromagnet. Since the sample is in ferrimagnetic state down to lowest temperature we belive we can use this expression to analyse our data below T_N. The parameters obtained from the fit for $\rho_a(T)$ are $\rho_0 = 680\ \mu\Omega$ cm, $a = 0.03\ \mu\Omega$ cm/K^2, $b = 6.2\ \mu\Omega$ cm/K^2 and $\Delta = 64$ K. Whereas the fit parameters for $\rho_b(T)$ are $\rho_0 = 70\ \mu\Omega$ cm, $a = 0.011\ \mu\Omega$ cm/K^2, $b = 1.23\ \mu\Omega$ cm/K^2 and $\Delta = 64.5$ K [5]. The important thing to note here is the value of Δ obtained for both the axes in almost same. So

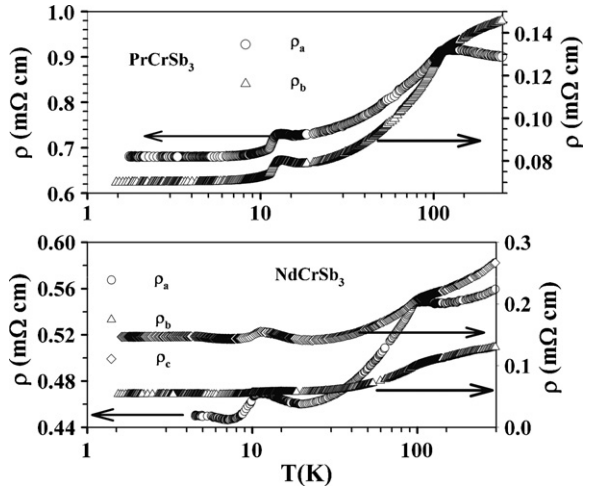

Fig. 3. The top panel shows $\rho(T)$ data for $PrCrSb_3$ sample along a- and b-axes. The inset of top panel is the low temperature fit of resistivity data (see text). The lower panel shows resistivity versus temperature data for $NdCrSb_3$ sample for current along a-, b- and c-axes.

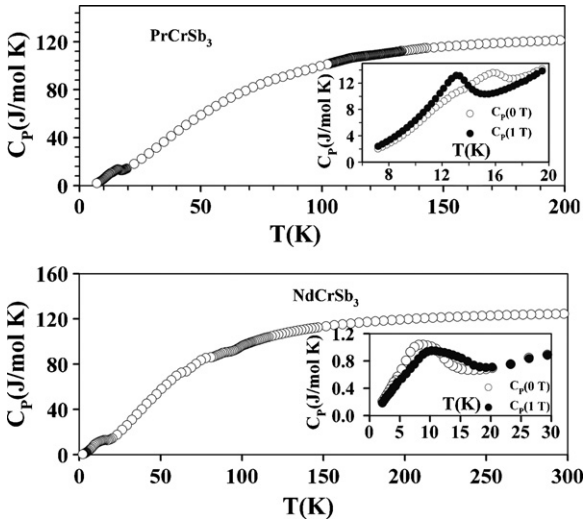

Fig. 4. The top(bottom) panel shows specific heat data for $PrCrSb_3$($NdCrSb_3$). Both the samples show two well-defined kinks in the $C_p(T)$ data at the two magnetic ordering temperatures. The insets of both panels show low temperature part of specific heat versus temperature data.

the idea of fitting low temperature resistivity data to the spin-wave gap expression was correct.

The lower panel of Fig. 3 shows the resistivity data along all three axes for $NdCrSb_3$. The sample exhibits anisotropy in resistivity with room temperature values of $\rho_a = 560\ \mu\Omega$ cm, $\rho_b = 148\ \mu\Omega$ cm and $\rho_c = 268\ \mu\Omega$ cm. Unlike large anisotropy observed in the resistivity data of $LaCrSb_3$, here we see, ρ_a/ρ_c is only of the factor of 2 at room temperature which increases to 3 at low temperatures ($T < 5$ K). However, the ratio ρ_a/ρ_b is 3.7 at room temperature and enhances to 10 below 5 K. The anomaly at the two magnetic transitions is clearly seen for all the axes. But unlike $PrCrSb_3$ we do not see here the gap in spin-wave spectrum.

The temperature dependence of the heat capacity $C_p(T)$ of $PrCrSb_3$ between 6 K and 200 K is shown in the upper panel of Fig. 4. Unlike $LaCrSb_3$ [6] we see a well-defined peak in the heat capacity data of $PrCrSb_3$ at $T_C = 112$ K. The peak at T_C gets smeared with the application of 1 T of field. The broadening of the heat capacity peak for $PrCrSb_3$ at T_C is supportive of the fact that Cr moments undergo ferromagnetic transition. We also see the low temperature kink in the heat capacity data at $T_N = 12$ K. This peak as seen in the inset of upper panel of Fig. 4 gets shifted to lower value of temperature with application of field implying that the magnetic ordering is AFM at this temperature.

The lower panel of Fig. 4 shows heat capacity $C_p(T)$ data for $NdCrSb_3$. We see a well-defined anomaly at $T_C = 100$ K, the Cr ordering temperature. But this anomaly is considerably weak as compared to that of $PrCrSb_3$. The anomaly at T_C gets smeared with application of field, again supporting the ferromagnetic nature of Cr ordering. The inset of lower panel of Fig. 4 shows low temperature anomaly in heat capacity data of $NdCrSb_3$. This kink appears due to magnetic ordering of Nd moments. The broadening of this kink with application of 1 T of field supports the fact that Nd orders ferromagnetically in $NdCrSb_3$ (which is further supported by the neutron data [7]) unlike $PrCrSb_3$ where Pr orders AFM.

4. Conclusion

To conclude, we have grown single crystals of the $PrCrSb_3$ and $NdCrSb_3$ by flux growth method and characterized them by X-ray, Laue back scattering, dc magnetic susceptibility, isothermal magnetization, resistivity and heat capacity (0 T and 1 T) measurements. All measurements confirm bulk ferromagnetic ordering of Cr moments below 112 K and 100 K for $PrCrSb_3$ and $NdCrSb_3$, respectively. The magnetic susceptibility χ follows modified Curie–Weiss behaviour above 200 K and the estimated effective moment comes out to be nearly equal to $4(5)\mu_B$/f.u. for Pr(Nd)$CrSb_3$ as compared to that of $3.01\mu_B$/f.u. for $LaCrSb_3$. The easy axis of magnetization for Cr moments continues to be *b*-axis for both the compounds as in the case of $LaCrSb_3$ and $CeCrSb_3$. R^{3+}–Cr^{3+} interaction gives a complex magnetic phase below T_C. This gives different signature of $\chi(T)$ along all the three axis. But unlike $CeCrSb_3$ in $PrCrSb_3$ and $NdCrSb_3$ we see a sharp magnetic ordering due to moments of Pr and Nd at $T_N = 12$ K and $T_C = 10$ K, respectively. The easy axis for magnetization for rare earth moment ordering is along *a*-axis for both the samples. But Pr orders AFM whereas Nd orders FM in the respective $RCrSb_3$ compound. The resistivity and heat capacity measurements for (Pr, Nd)$CrSb_3$ also show anomaly at these two ordering temperatures confirming our analysis of the magnetic properties of this system. We observe gap in the spin-wave spectrum below the AFM ordering of Pr spins in $PrCrSb_3$, this gap is absent in $NdCrSb_3$.

References

[1] M.J. Ferguson, R.W. Hushagen, A. Mar, J. Alloys Compd. 249 (1997) 191.
[2] D.D. Jackson, M. Torelli, Z. Fisk, Phys. Rev. B 65 (2002) 014421.
[3] D.D. Jackson, S.K. McCall, A.B. Karki, D.P. Young, Phys. Rev. B 76 (2007) 064408.
[4] M. Inamdar, A. Thamizhavel, S. Ramakrishnan, JMMM 320 (2008) 2766–2769.
[5] M. Inamdar, A. Thamizhavel, S. Ramakrishnan, Phys. Rev. B 77 (2008) 132410.
[6] E. Granado, et al., Phys. Rev. Lett. 89 (2002) 1072041.
[7] L. Deakin, M.J. Ferguson, A. Mar, J.E. Greedan, A.S. Mills, Chem. Mater. 13 (2001) 1407.